



# SUPRAMOLECULAR NANOCONTAINER WITH THE MITOCHONDRIA-TARGETING FUNCTION BASED ON A CALIXRESORCINE CAVITAND

Cite this: *INEOS OPEN*,  
2025, 8 (1–3), XX–XX  
DOI: 10.32931/ioXXXXXx

Y. E. Morozova,\*<sup>a</sup> A. M. Shumatbaeva,<sup>b</sup> Z. R. Gilmullina,<sup>a</sup> A. P. Lyubina,<sup>a</sup>  
S. K. Amerhanova,<sup>a</sup> A. D. Voloshina,<sup>a</sup> V. V. Syakaev,<sup>a</sup> and I. S. Antipin<sup>b</sup>

<sup>a</sup> Arbuzov Institute of Organic and Physical Chemistry, FRC Kazan Scientific Center  
of the Russian Academy of Sciences, ul. Arbuzova 8, Kazan, 420088 Russia  
<sup>b</sup> Kazan Federal University, ul. Kremlevskaya 18, Kazan, 420008 Russia

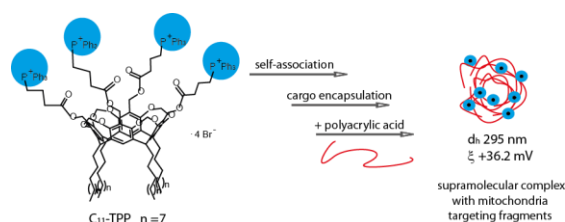
Received 07 October 2024,  
Accepted 2 November 2024

<http://ineosopen.org>

## Abstract

To create a mitochondria-targeted drug delivery system (MT DDS), a calixresorcine cavitand modified with triphenylphosphonium units (C<sub>11</sub>-TPP) and its polymer complex with polyacrylic acid (PAA) were synthesized. An optimal composition of the polymer complex and its parameters were found. It was shown that PAA reduced the hemotoxicity of C<sub>11</sub>-TPP and its toxicity to normal cells (Chang liver). However, the toxicity of C<sub>11</sub>-TPP+PAA complex against tumor cells (M-HeLa) was higher than that of the cavitand. Moreover, the mitochondria-dependent apoptotic pathway of M-HeLa cells was found in the presence of C<sub>11</sub>-TPP+PAA complex, indicating its potential as MT DDS.

**Key words:** calixresorcine, mitochondria-targeted drug delivery system, polymer complex.



## Introduction

As is known, drug delivery systems (DDSs) are a valuable tool for improving patient treatment and reducing the risk of adverse effects [1]. At the same time, the development of DDSs which can carry target ligands to enhance the specificity of delivery has become increasingly important [2].

Among them, the DDSs oriented towards intracellular specificity, such as DDSs bearing mitochondria-targeted (MT) ligands, hold great promise. Their action is based on the highly negative charge of the mitochondria membrane in cancer cells, which can provide the effectiveness of the MT DDS [3]. For example, triphenylphosphonium (TPP) derivatives can target mitochondria due to their delocalized charge and lipophilic nature [4].

One of the ways to obtain effective and inexpensive DDSs is the use of amphiphilic molecules that can self-organize, such as amphiphilic calixresorcine cavitands. Calixresorcines and their cavitands are receptor molecules that can be easily functionalized [5].

In order to obtain MT DDS, we modified a calixresorcine cavitand with TPP units and then obtained a supramolecular polymer–cavitand complex. The production of these complexes is one of the ways to optimize the sizes of DDS [6] in order to meet the requirements of the enhanced permeability and retention (EPR) effect [7]. Thus, our goal was to synthesize a cavitand bearing TPP units and to create a nanoscale polymer complex, as well as to investigate their *in vitro* toxicity.

Some inspiring examples of mitochondria-targeted systems based on cucurbiturils and cyclodextrins are presented in the Electronic Supplementary Information (ESI).

## Results and discussion

A new tetraundecylcalixresorcine cavitand bearing TPP units (Fig. 1) was synthesized from methylhydroxo-substituted cavitand and 3-(carboxypropyl)triphenylphosphonium bromide by the Steglich esterification. The synthetic procedure is described in the ESI. The structure of C<sub>11</sub>-TPP was confirmed by the <sup>1</sup>H and <sup>13</sup>C NMR spectra, IR spectrum (Figs. S1–S3 in the ESI) and elemental analysis data.

The investigation of C<sub>11</sub>-TPP+PAA polymer complex formation was started with the determination of the optimal C<sub>11</sub>-TPP/PAA molar ratio using the continuous variations method (Job's plot method) by the variation of molar fraction ( $\chi$ ) of the components from 0 to 1 in a solution with a constant concentration of 1 mM (in a solution of H<sub>2</sub>O–DMSO 95/5 (v/v); for details, see the ESI and Table S1). The size ( $d_h$ ) and electrokinetic potential ( $\xi$ ) of the solutions were analyzed (Figs. S4–S6 in the ESI).

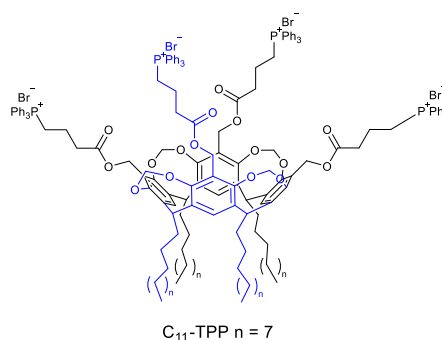


**Figure 1.** Structure of C<sub>11</sub>-TPP.

In PAA individual solution, the particles with  $d_h$  of 342 nm (PDI 0.366) and  $\xi$  of  $-34.2$  mV were observed. The largest size of C<sub>11</sub>-TPP+PAA particles was observed at  $\chi(\text{C}_{11}\text{-TPP}) = 0.1$  due to the charge compensation (1484 nm, +10 mV). An increase in the C<sub>11</sub>-TPP fraction led to a decrease in the size and a gradual increase in the value of  $\xi$  (Fig. S6 in the ESI). As a result, a 0.5/0.5 molar ratio was chosen. The  $d_h$  value of C<sub>11</sub>-TPP/PAA 0.5/0.5 particles in PB solution (pH 7.4) was 295 nm (PDI 0.214, Fig. 2).

The macrocycle–polymer complex can be formed primarily due to electrostatic interaction [6]. To confirm PAA–C<sub>11</sub>-TPP association, IR spectroscopy, fluorimetry, and conductometry were used. In the IR spectrum, the C=O absorption bands of PAA and the cavitand are overlapped, and only minor shifts of C=O and C–O–C bands of C<sub>11</sub>-TPP are observed, which might indicate the formation of hydrogen bonds with COOH groups of PAA or with water molecules (Fig. S3 in the ESI). According to the results of the fluorometric analysis, in the presence of PAA, the critical association concentration (*cac*) value of C<sub>11</sub>-TPP shifts from 0.095 to 0.050 mM (Figs. S7 and S8 in the ESI), which can be explained by the formation of C<sub>11</sub>-TPP+PAA complex. The data of conductivity isotherms are more informative (Fig. S9 in the ESI) and demonstrate that PAA increases the *cac* value of C<sub>11</sub>-TPP (from 0.120 to 0.153 mM), indicating a strong affinity of the cavitand molecules to the PAA surface. According to these data, it can be proposed that at 0.5/0.5 C<sub>11</sub>-TPP/PAA molar ratio, the cavitand self-associates absorb on PAA molecules (Fig. 2b). The encapsulation and release ability of the complex were studied using optical probe fluorescein (FI) (for details, see the ESI). A slow rate of the FI release was observed, with 24% released FI in 8 h (Fig. S10 in the ESI). Therefore, passive diffusion of the drug from the studied complex may be considered.

The *in vitro* toxicity of C<sub>11</sub>-TPP, PAA, and the complex were studied (Table 1). PAA was found to be low toxic. The toxicity of the cavitand in the complex against erythrocytes and normal cells reduced, while the toxicity against tumor cells increased. The ability of the cavitand and the complex to decrease the mitochondrial potential ( $\Delta\Psi_m$ ) of M-HeLa cells and to induce their apoptosis through the intrinsic mitochondrial pathway was investigated by flow cytometry using JC-10 dye. In normal cells with a high  $\Delta\Psi_m$  value, JC-10 forms aggregates with red fluorescence. When  $\Delta\Psi_m$  decreases due to apoptosis, JC-10 becomes uniformly distributed throughout the cell in a monomeric form with green fluorescence. The analysis of the red/green fluorescence ratio allows to detect apoptosis onset. The results obtained suggest that C<sub>11</sub>-TPP is able to reduce  $\Delta\Psi_m$  and maintain this effect in the complex (Fig. S11 in the ESI). The most significant decrease in the value of  $\Delta\Psi_m$  in M-HeLa cells was observed for C<sub>11</sub>-TPP+PAA complex at 8  $\mu\text{M}$  (Fig. 3).

**Table 1.** Hemolytic activity and cytotoxicity of C<sub>11</sub>-TPP, PAA, and the resulting complex

	HC <sub>50</sub> , $\mu\text{M}$	IC <sub>50</sub> , $\mu\text{M}$	
		Chang liver	M-HeLa
C <sub>11</sub> -TPP	30.1 $\pm$ 1.8	12.6 $\pm$ 1.1	18.4 $\pm$ 1.7
PAA	>300	121.2 $\pm$ 2.5	162.0 $\pm$ 1.2
Complex	35.8 $\pm$ 2.8	14.2 $\pm$ 2.1	8.0 $\pm$ 0.6

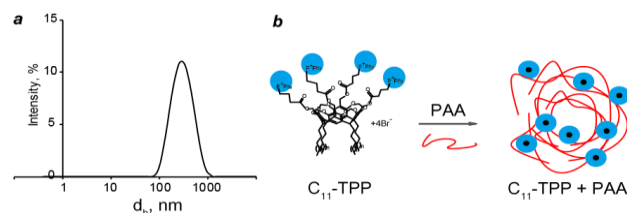


**Figure 2.** Intensity of particle size distribution of C<sub>11</sub>-TPP+PAA (0.5/0.5) in PB–DMSO solution (95/5 v/v), pH 7.4 (a); the proposed scheme of C<sub>11</sub>-TPP+PAA complex formation (b).

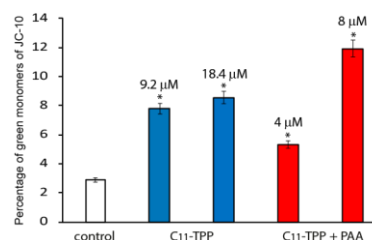


**Figure 3.** Percentage of cells with green fluorescence of JC-10 after treatment of M-HeLa cells with the samples. The values are presented as the mean  $\pm$  SD (standard deviation). The experiments were performed in triplicate.  $P < 0.01$  compared to the control.

## Conclusions

Hence, the cavitand bearing TPP units was synthesized that exhibit toxicity against M-HeLa cancer cells *via* apoptosis through the intrinsic mitochondrial pathway. It was shown that it forms a complex with PAA, which, at the C<sub>11</sub>-TPP/PAA molar ratio of 1/1, has a size of 295 nm (PDI 0.214) in PB pH 7.4 and zeta potential of +36.2 mV, and can serve as a nanocontainer for cargo delivery. It was also demonstrated that C<sub>11</sub>-TPP+PAA complex has lower toxicity towards red blood cells and normal liver cells compared to the cavitand. However, the toxicity of the complex towards M-HeLa is higher than that of the cavitand, indicating its potential to serve as MT DDS.

## Acknowledgements

This work was performed within the government assignment for the FRC Kazan Scientific Center of the Russian Academy of Sciences. The authors are grateful to the Assigned Spectral-Analytical Center of the FRC Kazan Scientific Center of the Russian Academy of Sciences.

## Corresponding author

\* E-mail: moroz@iopc.ru (Y. E. Morozova).

## Electronic supplementary information

Electronic supplementary information (ESI) available online: the synthesis of C<sub>11</sub>-TPP, <sup>1</sup>H and <sup>13</sup>C NMR spectra of C<sub>11</sub>-TPP, IR spectra of C<sub>11</sub>-TPP, PAA and the resulting complex, DLS, fluorescence and conductivity data, the data of FI release, the *in vitro* toxicity and flow cytometry data. For ESI, see DOI: 10.32931/ioXXXXX.

## References

1. B. Akash, S. Ravindranath, *J. Drug Delivery Ther.*, **2019**, 9, 517–521. DOI: 10.22270/jddt.v9i3.2610
2. A. Prajapati, S. Rangra, R. Patil, N. Desai, V. G. S. S. Jyothi, S. Salave, P. Amate, D. Benival, N. Kommineni, *Receptors*, **2024**, 3, 323–361. DOI: 10.3390/receptors3030016
3. D. Singh, *Mitochondrion*, **2024**, 74, 101826. DOI: 10.1016/j.mito.2023.101826
4. S. Batheja, S. Gupta, K. K. Tejavath, U. Gupta, *Drug Discovery Today*, **2024**, 29, 103983. DOI: 10.1016/j.drudis.2024.103983
5. J. A. Gajjar, R. H. Vekariya, H. M. Parekh, *Synth. Commun.*, **2020**, 50, 2545–2571. DOI: 10.1080/00397911.2020.1766080
6. Ju. E. Morozova, A. M. Shumatbaeva, I. S. Antipin, *Colloid J.*, **2022**, 84, 530–545. DOI: 10.1134/S1061933X2270003X
7. J. Wu, *J. Pers. Med.*, **2021**, 11, 771. DO: 10.3390/jpm11080771